Asymmetric Centrosome Maturation in the Early *C. elegans* Embryo Revealed by Multi-scale Microscopy and Mathematical Modeling

Shayne M. Plourde[1], Natalia Kravtsova[2], Adriana Dawes[1,2]
[1] The Ohio State University, Department of Molecular Genetics, Columbus, Ohio [2] The Ohio State University, Department of Mathematics, Columbus, Ohio

My personal website:
shayne-falco.github.io

INTRODUCTION

The process by which cells position their centrosomes is critically important for proper cell divisions[1,2]. Centrosomes are the main microtubule organizing centers of the cell and abnormal positioning during cell division is one potential cause leading to cancer metastasis[3].

Microtubule (MT) Array Asymmetry in *C. elegans*

We use *C. elegans* as a model for asymmetric cell division and centrosome placement because the steps leading up to the first asymmetric cell division are tightly regulated[4] (Fig. 1a). Our lab previously reported an asymmetry in the size and density of the MT arrays from the two centrosomes during the first cellular division of the *C. elegans* embryo[5]. The source of this asymmetry is currently unknown.

We analyze the fluorescence intensity of a GFP tagged AIR-1, a factor found in the centrosome that is required for microtubule nucleation in both centrosomes.

- Leading centrosome found in the anterior (larger) cell.
- Lagging centrosome found in the posterior (smaller) cell.

Figure 1. Imaging Fluorescent Centrosomes Leading up to the First Division of *C. elegans*

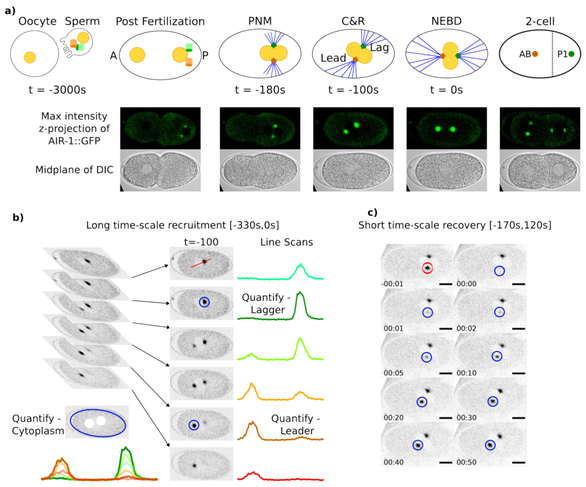

Figure 1. a) The steps leading up to first division are fertilization, pronuclear meeting (PNM), centration and rotation (C&R), and Nuclear envelope breakdown (NEBD). NEBD is used to mark a time of 0 seconds as it coincides with when the centrosomes have been properly placed for cell division. C) Recruitment was quantified every 10 seconds from 330 seconds before NEBD to 0 seconds. Blue circles represent the quantified regions representing the middle of the centrosome and the average of all stacks with centrosomes masked out representing the cytoplasmic fluorescence intensity. c) Recovery was quantified immediately after pronuclear meeting (PNM) every second for 50 seconds.

RESULTS

Figure 2. Asymmetric Centrosome Recruitment and Recovery Revealed by Precise Quantification

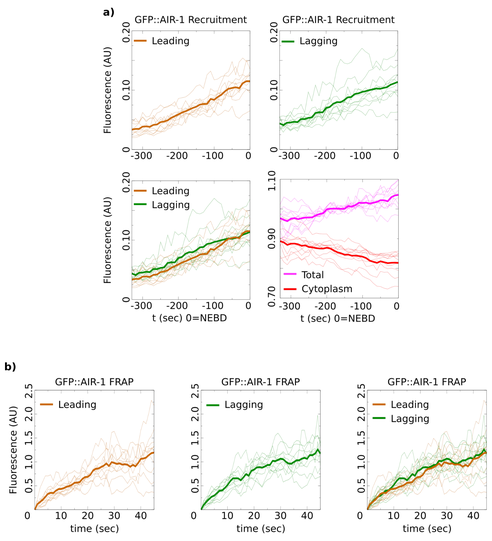

Figure 2. a) Leading centrosome, lagging centrosome, cytoplasmic, ad the total cell fluorescence intensities of GFP::AIR-1 were precisely quantified and then normalized. The average intensity of the lagging centrosome was observed to be higher than that of the leading centrosome. b) Fluorescence recovery after photobleaching (FRAP) was recorded for 10 leading and 10 lagging centrosomes and normalized as per standard protocols[6]. The final concentrations of the recovery curves were similar for both compartments.

Statistical Analysis Shows Asymmetries

Our recently published Gromov-Wasserstein based distance metric was used to identify any potential differences between the shapes of the calculated recruitment and recovery curves[7].

The recruitment did not show a difference between leading and lagging centrosomes indicating that their dynamics were overall similar. However, the recruitment in the lagging centrosomes is greater than the leading centrosome until ~-50s which would not be captured by this analysis (Fig. 2a).

The FRAP curve analysis identified distinct recovery dynamics between the two centrosomes even though the curves recovered to the same final amount (Fig. 2b).

MATHEMATICAL MODELING

To uncover potential mechanisms responsible for the reported centrosomal dynamics and the differences between centrosomes, we turned to mathematical modeling. A 3-compartment model representing the two centrosomes as well as the cytoplasm was constructed to simulate a maturation factor's recruitment and recovery in a one-cell embryo (Fig. 3).

Figure 3. 3-Compartment Model of Centrosome Recruitment and Recovery After Photobleaching

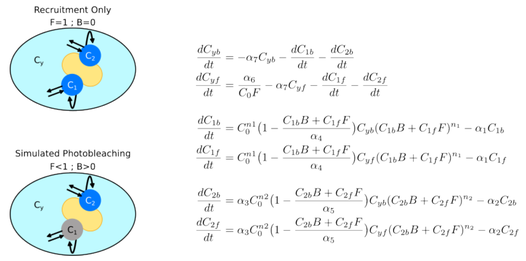

$$\frac{dC_{yb}}{dt} = -\alpha_7 C_{yb} - \frac{dC_{1b}}{dt} - \frac{dC_{2b}}{dt}$$
$$\frac{dC_{yf}}{dt} = \frac{\alpha_6}{C_0 F} - \alpha_7 C_{yf} - \frac{dC_{1f}}{dt} - \frac{dC_{2f}}{dt}$$
$$\frac{dC_{1b}}{dt} = C_0^{n_1}\left(1 - \frac{C_{1b}B + C_{1f}F}{\alpha_4}\right) C_{yb}(C_{1b}B + C_{1f}F)^{n_1} - \alpha_1 C_{1b}$$
$$\frac{dC_{1f}}{dt} = C_0^{n_1}\left(1 - \frac{C_{1b}B + C_{1f}F}{\alpha_4}\right) C_{yf}(C_{1b}B + C_{1f}F)^{n_1} - \alpha_1 C_{1f}$$
$$\frac{dC_{2b}}{dt} = \alpha_3 C_0^{n_2}\left(1 - \frac{C_{2b}B + C_{2f}F}{\alpha_5}\right) C_{yb}(C_{2b}B + C_{2f}F)^{n_2} - \alpha_2 C_{2b}$$
$$\frac{dC_{2f}}{dt} = \alpha_3 C_0^{n_2}\left(1 - \frac{C_{2b}B + C_{2f}F}{\alpha_5}\right) C_{yf}(C_{2b}B + C_{2f}F)^{n_2} - \alpha_2 C_{2f}$$

Figure 3. 3-compartment mathematical model of a maturation factor that can localize to the simulated cytoplasm (C_y), or the two centrosome compartments (C_1, C_2). To incorporate the ability to photobleach the model factor we track both a fluorescent version (f) and a bleached version (b) of the maturation factor. Dynamics for the system accounted for both version of the factor to be as biologically relevant as possible. b) Model equations with a dynamic cytoplasm and centrosome compartment that have a carrying capacity, cooperativity, and basal gain and loss terms.

Figure 4. Parameter Sets that Recapitulate *in vivo* Recruitment & Recovery Data

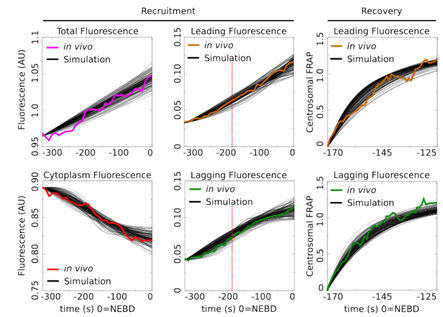

Figure 4. Using a parameter search based on our MCMC method[8] we were found 112 parameter sets that fit the model's maturation factor to the observed AIR-1::GFP data. These parameter sets all independently fit to the 6 data curves with a low error as calculated by the sum of absolute differences.

Parameter Space of the Model Reveals Structural Features of the Centrosomes

There are three features that define the structural dynamics of the centrosome compartments in the model. The cooperativity, carrying capacity, and the ratio of the on rate to the off rate. Plotting all 112 parameter sets on a 3D plot with these features as the axis and differentiating the leading from the lagging centrosome revealed a high level of restriction to the location of possible parameters (Fig. 5).

Figure 5. Parameter Space Shows Asymmetry in Centrosome Structural Composition

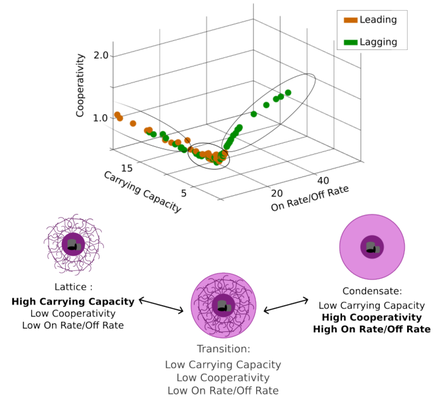

Figure 5. The centrosome compartment parameters represent the overall structural composition of the centrosomes. To visualize the possibilities revealed by our parameter search we plotted all parameter sets on 3D plot with axis for cooperativity, carrying capacity, and the ratio of the on rate to the off rate. We saw that the parameters were confined to a well-defined region of this parameter space. This region is defined by two arms, one with high levels of carrying capacity and one with high cooperativity and on rate to off rate ratio. There is a region connecting these two arms where all 3 parameter values are relatively low.

DISCUSSION

Early embryo *C. elegans* Centrosomes are asymmetric.

Combining a precise quantification of a factor required for MT nucleation and mathematical modeling we found that the leading and the lagging centrosomes have different dynamics.

Emergent Centrosome Structural Asymmetry

The two extremes of the parameter space coincide with previously published biological hypotheses of centrosome structure (Fig. 5b). Our model gives these three structures a common model and may explain the recently reported progression of centrosomes from a liquid condensate state to a more ridged lattice state[9].

FUTURE DIRECTIONS

Expanding *in vivo* & *in silico* Work to New Factors

To extend these results we will be investigating the recruitment, recovery, and maturation of more centrosomal factors. Of particular interest will be factors granting the centrosome its strength. With a larger data set we will also be able to expand our mathematical model to include more terms and more dynamic interactions.

REFERENCES

1. Meraldi et al., 2016, Chromosome Res. 24:19-34
2. Yamashita et al., 2009, Frontiers in Bioscience, (14):3003
3. Pancione et al., 2021, Biomolecules, 11(5): 629
4. Rose et al., 2014, WormBook, Dec 30:1-43.
5. Coffman et al., 2016, MBOC, 27(22):3550–3562.
6. Kress et al., 2013, JCB, 201(4):559-575
7. Kravtsova et al. 2023, Bulletin of Mathematical Biology 85(8)
8. Kravtsova et al. 2023, Scientific reports 13(1), 16285.
9. Woodruff 2021, Curr Opin Struct Biol. 66:139-147

AKNOWLEDGMENTS

We would like to thank our funding agencies, NSF & NIH, as well as The Ohio State University and the MCDB graduate program

THE OHIO STATE UNIVERSITY

MCDB MOLECULAR, CELLULAR, AND DEVELOPMENTAL BIOLOGY